

# Structural Study of Fe/Al MLS as a Function of Fe Film Thickness

R. Brajpuriya

Amity Institute of Nanotechnology, Amity University Haryana, Gurgaon, India

**Abstract:** The paper presents surface and interface structural study of electron beam evaporated  $[Fe (40\text{\AA} - 10\text{\AA})/Al (10\text{\AA})]_{\times 15}$  thin multilayer structures (MLS). The structural studies show significant amount of intermixing between the layers during growth for lower thickness of Fe layer ( $\leq 20\text{\AA}$ ), indicating the loss of periodicity at these thicknesses i.e. the prepared layers are not continuous and they are far away from the percolation threshold. These structures appear like a composite film consisting clusters of Fe and Al matrix. However, at higher Fe layer thickness ( $\geq 30\text{\AA}$ ), the presence of first order Bragg diffraction in reflectivity patterns demonstrates the evaluation of a better-MLS as compared to lower Fe layer thickness. AFM and resistivity measurements also support the above results.

**Keywords:** Fe/Al multilayers GIXRD; GIXRR; AFM; Thickness

## 1. Introduction

Metallic multilayer films with manufactured periodicity obtained by alternate deposition of ferromagnetic and non-magnetic films show an improvement of magnetic properties, most suitable for high density magnetic recording [1, 2]. Among many MLS, Fe/Al bilayer and ML systems also have the potential to be used as thin film magnetic head for recording media, and it has been shown to possess excellent soft magnetic properties required for such use [3, 4]. However, the fundamental magnetic properties of these MLS are largely different from their bulks. It has been observed that the structural parameters such as thickness, periodicity and the nature of interfaces formed during deposition greatly affect these interesting properties [5-7]. In various cases, it is found that reaction and interdiffusion phenomena at interfaces during growth causes a loss of periodicity below a certain thickness, which severely modifies the structural and magnetic properties of these multilayers. Under such conditions, one needs a careful characterization of these structures in order to understand the role played by various micro-structural parameters, and in interpreting the different properties displayed by them. Therefore, in the present paper we have systematically carried out the structural and morphological studies of Fe/Al bilayers (BL) and multilayers (ML). The combination of distinct non-destructive techniques such as grazing incidence x-ray diffraction (GIXRD), x-ray reflectivity (GIXRR), atomic force microscopy (AFM), and four-probe resistivity were used to characterize the same.

## 2. Experimental Details

For the present study e-beam evaporation method is used to deposit  $[Fe (40\text{\AA} - 10\text{\AA})/Al (10\text{\AA})]_{\times 15}$  MLS. The samples were prepared at RT under UHV conditions keeping  $0.1\text{\AA}/s$  deposition rate for both layers of Fe and Al. A capping layer of Al ( $25\text{\AA}$ ) was deposited on top to avoid oxidation of MLS. All ML and bilayer (BL) samples were synthesized in a single run. GIXRD, GIXRR and AFM techniques were used to obtain the micro-structural and morphological information of the samples. The GIXRD and GIXRR

measurements were carried out at a wavelength ( $\lambda$ ) of  $1.542\text{\AA}$ , operated at 40 KV and 30 mA. Morphological (AFM) measurements (Digital Instruments Nanoscope III) were carried out on bilayer samples in the contact mode. To save the samples from the contaminations the images were collected just after the samples were taken out from the synthesis chamber. The four probe method is employed to obtain the resistivity data.

## 3. Results and Discussion

Figure. 1 depicts the thickness (Fe) dependent GIXRD patterns of pristine  $[Fe/Al]_{\times 15}$  MLS. Diffraction patterns show that in all the cases samples was textured along Fe (110) direction. One can also notice that no peaks corresponding to Al were found proving that the prepared Al layer ( $10\text{\AA}$ ) is amorphous or nanocrystalline in nature. In case of  $[Fe (40\text{\AA})/Al (10\text{\AA})]_{\times 15}$  MLS, the  $2\theta (44.62^\circ)$  value of Fe (110) peak is found to be close to bulk Fe ( $44.67^\circ$ ) [8]. However, as the thickness of Fe layer decreases the peak intensity as well as  $2\theta$  values decreases i.e. the peak shifts towards lower  $2\theta$  values. It is also found that peaks broaden with decrease in Fe layer thickness. The variation in the peak position and shape can be interpreted as follows: (i) increase in interplanar spacing 'd' due to large internal stress in the Fe layers introduced by adjacent Al layers, and their (ii) intermixing at the interface during growth resulting iron aluminide phase formation. Grain size of Fe crystallites is a critical structural parameter to modify the magnetic properties, together with the grain orientation, which controls the magnetic anisotropy. Therefore, using Scherrer formula we have determined the average particle size from the recorded GIXRD patterns as shown in table 1. It is found that the average particle size decreases linearly with decreasing Fe layer thickness. This indicates that large and more oriented crystallites of Fe were grown in case of MLS with greater  $d_{Fe}$ .

However, for lower Fe layer thickness it is appeared to be composed of nano-crystallites Fe and Al grains, leading to a distorted Fe lattice structure. Table 1 also shows the measured d spacing value as a function of Fe layer thickness.

Volume 5 Issue 6, June 2016

[www.ijsr.net](http://www.ijsr.net)

Licensed Under Creative Commons Attribution CC BY

One can clearly see that d spacing value decreases with increase in layer thickness of Fe. As the Fe layer thickness increases to 40Å the d value moving towards the bulk d value of Fe. The variation in d spacing values with Fe layer thickness indicates that the stresses were presents in the prepared MLS, which released as Fe layer thickness increase to form more continuous and ordered layers.

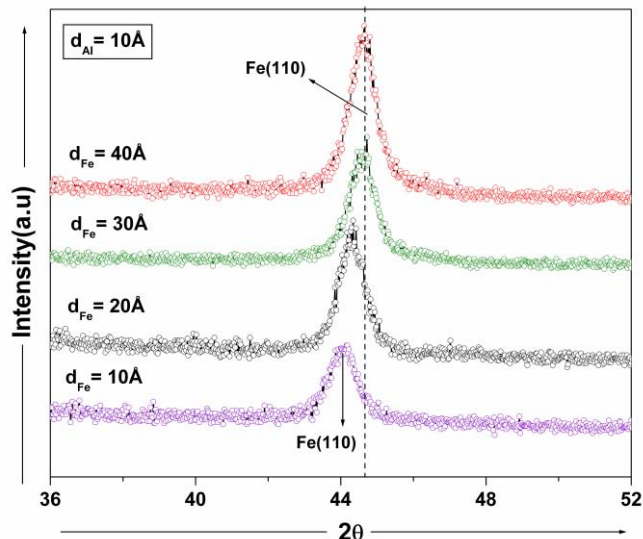


**Figure 1:** GIXRD patterns of as deposited  $[Fe(d_{Fe})/Al(10\text{\AA})]_{x15}$  MLS.

**Table 1:** Values obtained from GIXRD, GIXRR, AFM and resistivity measurements as a function of  $d_{Fe}$

$d_{Fe}$ (Å)	$L$ (Å)	$D_0$ (Å)	$\sigma$ (Å)	$\rho$ ( $\mu\Omega cm$ )
10	75	2.05	13.5	127
20	82	2.04	22.9	91
30	86	2.03	18.6	34
40	97	2.03	16.2	20

Figure. 2 depicts the GIXRR patterns of the corresponding pristine  $[Fe/Al]_{x15}$  MLS. The reflectivity patterns shown in fig. 2a and 2b corresponding to  $d_{Fe}$  (10 Å) and  $d_{Fe}$  (20 Å) are not similar to typical patterns of a multilayer structure. In both the present cases author do not observed well defined Bragg peaks received due to the periodicity of MLS, implying a considerable amount of intermixing at the interface during growth. Indeed this is expected because both the layers involved here are very thin and possibly may not be sufficient thick enough to form continuous and ordered layers that would lead to well defined interfaces. This is what our XRD results also shown. The prepared structures in these cases mostly displays a composite structure consisting of Fe and Al giving rise to large roughness values (see table. 1). Whereas at higher  $d_{Fe}$ , the presence of first order Bragg reflection, indicates the formation of a better layered structure (see fig. 2c and 2d). The calculated modulation wavelengths of 38.5Å in case of  $d_{Fe}=30$  Å and 47.3 Å in case of  $d_{Fe}=40$  Å matches reasonably well with the desired bilayer periodicity. In these two cases, the reflectivity patterns were fitted by assuming two layers i.e. elemental Fe layer along with an intermix FeAl layer. The total thickness determined for the

lower thickness samples also matches well with the prepared thicknesses when they are considered as a composite single layer structure.

In every MLS, bilayer structure (BLS) plays a very decisive role for which MLS is prepared and therefore, under similar conditions Fe/Al bilayer samples were made and conducted morphological studies on them. Fig. 3 depicts the two-dimensional morphological images of  $[Fe(10\text{\AA})/Al(10\text{\AA})]$  and  $[Fe(40\text{\AA})/Al(10\text{\AA})]$  bilayer samples. It is seen that at 10Å Fe layer thickness (fig. 3(a)) bilayer structure is not continuous and presenting an island like growth with large variation in particle shape and sizes. It looks like that Fe clusters are embedded in the matrix of Al and as a result large rms surface roughness value is found in this case. Table. 1 displays the variation in surface roughness as a function of  $d_{Fe}$ .

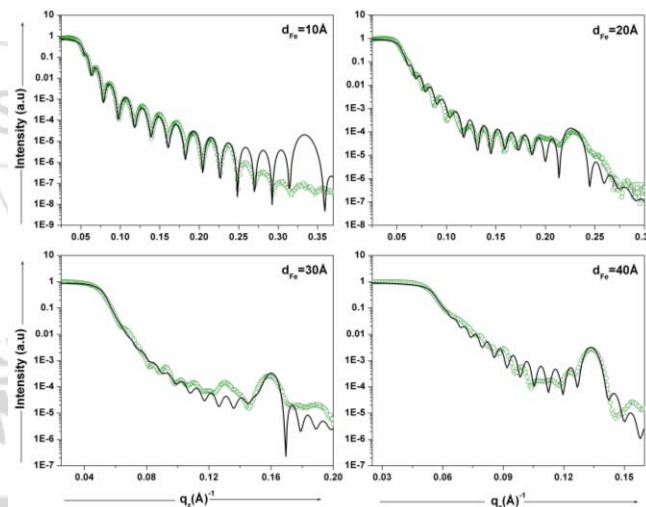


**Figure 2:** GIXRR patterns of the as prepared  $[Fe(d_{Fe})/Al(10\text{\AA})]_{x15}$  MLS.

The rms roughness has been calculated by taking the average over at least 5 regions of area  $1 \times 1 \mu m$ . As the thickness of Fe layer increases, surface roughness increases to a particular layer thickness and thereafter decreases, and has maximum roughness for  $d_{Fe}=20$  Å. The average roughness found to be in this case is 22.9 Å. So one can understand the obtained reflectivity patterns by seeing the above AFM images why a well-defined MLS is not observed at lower Fe layer thicknesses. However, as the Fe layer thickness is increased further to  $\geq 30$  Å, the separation of these features decreases and show the formation of more continuous and denser layers compared to the above-mentioned cases and as a result the value of surface roughness decreases to 16.2 Å. This is in correlation with the reflectivity patterns which also shows the formation of a better layered structure at these thicknesses. Hence, these images provide us more clear information about different stages of growth as the thickness of Fe layer is increases from 10 Å to 40 Å.

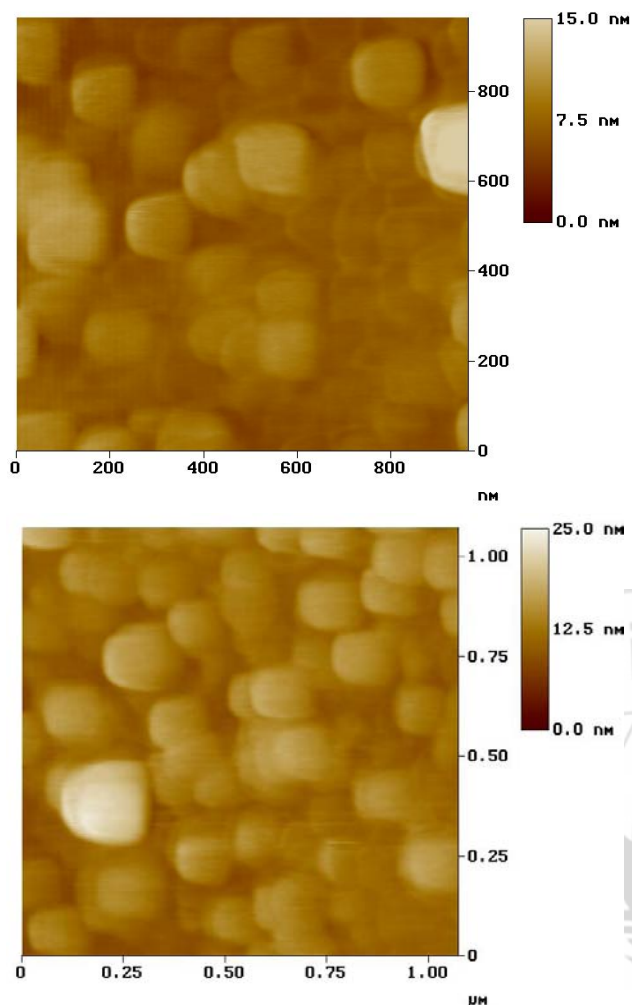


**Figure 3:** Two-dimensional AFM images of  $[\text{Fe}(10\text{\AA})/\text{Al}(10\text{\AA})]$ , and  $[\text{Fe}(40\text{\AA})/\text{Al}(10\text{\AA})]$  bilayer samples

Table 1 displays the thickness dependent variation in resistivity value. It is clear from the table that the resistivity decreases rapidly as the Fe layer thickness increases. This is similar to what happen in case of a single layered metallic film [9]. Thus, from the resistivity measurements it is possible to derive the structure of each layer in the prepared MLS. The table also informed that resistivity is maximum for a lower Fe layer thickness, implying that the prepared layers are not continuous and they are far away from the percolation threshold. The GIXRD, GIXRR and AFM measurements certainly confirm the above results. However with increase in Fe layer thickness to  $\geq 30 \text{ \AA}$ , the resistivity value falls to a minimum marking the development of more continuous growth in accordance with earlier structural studies. However, the value of resistivity is still higher in comparison to their bulk counter parts and is mainly associated to structural disorders and interdiffusion leading to alloying at the interfaces during growth.

#### 4. Conclusion

The paper shows the effect of Fe layer thickness on the surface and interface structural properties of Fe/Al MLS keeping Al layer thickness constant. At lower  $d_{\text{Fe}}$ , the structural and morphological measurements showed

significant amount of intermixing due to discontinuous growth of Fe and Al layers and interdiffusion at the interface during growth. At lower Fe layer thicknesses, the prepared layers are not continuous and looks like a composite single layer structure consisting of Fe clusters embedded in a matrix of an Al.

#### References

- [1] R Brajpuriya, Journal of Applied Physics 107 (2010) 083914.
- [2] R. Nakatani et al. J. Appl. Phys. 66 (1989) 4338.
- [3] R Brajpuriya, and T Shripathi, Applied Surface Science 255 (2009) 6149.
- [4] G. V. Sudhakar Rao, A. K. Bhatnagar, F. S. Razavi, J. Magn. Magn. Mater, 247 (2002) 159.
- [5] F. Albertini, G. Carlotti, F. Carlotti, F. Casoli, G. Gubbiotti, H. Koo, R. D. Gamez, J. Magn. Magn. Mater, 240 (2002) 526.
- [6] E. Fonda, A. Traverse, J. Magn. Magn. Mater, Vol. 268 (2004) 292.
- [7] R Brajpuriya, S Tripathi, A Sharma, SM Chaudhari, T Shripathi, N Lakshmi, Journal of Vacuum Science & Technology A 26 (2008) 571.
- [8] JCPDS file No 4-787 and 6-696.
- [9] Y. Kozono, M. Komuro, S. Narishige, M. Hanazaono, Y. Sugita, J. Appl. Phys. 61 (1987) 4311.